Astronomy & Astrophysics manuscript no. Rotation
October 1, 2014

Steps toward a high precision solar rotation profile: Results from SDO/AIA coronal bright point data

D. Sudar[1], I. Skokić[2], R. Brajša[1], and S. H. Saar[3]

[1] Hvar Observatory, Faculty of Geodesy, Kačićeva 26, 10000 Zagreb, Croatia
[2] Cybrotech Ltd, Bohinjska 11, 10000 Zagreb, Croatia
[3] Harvard-Smithsonian Center for Astrophysics, 60 Garden Street, Cambridge, MA 02138, USA

Release October 1, 2014

ABSTRACT

Context. Atmospheric Imaging Assembly is an instrument on-board Solar Dynamics Observatory satellite. It is capable of detecting and identifying coronal bright points in the solar corona.
Aims. We present the results of solar differential rotation profile by tracing coronal bright points detected by Atmospheric Imaging Assembly. We also investigated problems related to detection of coronal bright points resulting from instrument and detection algorithm limitations.
Methods. To determine the positions and identification of coronal bright points we used the segmentation algorithm. Linear fit of central meridian distance and latitude versus time was utilised to obtain related velocities of the tracer.
Results. We obtained 906 velocity measurements in time interval of only 2 days. Differential rotation profile can be expressed as $\omega_{rot} = (14.47 \pm 0.10 + (0.6 \pm 1.0)\sin^2(b) + (-4.7 \pm 1.7)\sin^4(b))^\circ \mathrm{day}^{-1}$.
Conclusions. Data and methods presented in this paper show a great potential to obtain very accurate velocity profiles, both for rotation and meridional motion and, consequently, Reynolds stresses. The amount of coronal bright point data that could be obtained from this instrument should also provide a great opportunity to study changes of velocity patterns with a temporal resolution of only a few months. Other possibilities are studies of evolution of coronal bright points and proper motions of magnetic elements on the Sun.

Key words. Sun: rotation - Sun: corona - Sun: activity

1. Introduction

We present the results of solar rotation profile obtained by tracing coronal bright points (CBPs) which were observed by Atmospheric Imaging Assembly (AIA) instrument on board Solar Dynamics Observatory (SDO) satellite (Lemen et al. 2012).

The most frequently used and oldest tracer of solar differential profile are sunspots (Newton & Nunn 1951; Howard et al. 1984; Balthasar et al. 1986; Brajša et al. 2002a). One of the advantages of using sunspots is very long time coverage. On the other hand, there are numerous disadvantages: sunspots have complex and evolving structure, their distribution in latitude is highly non-uniform and it does not extend to higher solar latitudes. Number of sunspots is also highly variable during the solar cycle which makes measurements of solar differential rotation profile almost impossible in the minimum of solar activity.

CBPs are more uniformly distributed in latitude and are numerous in all phases of the solar cycle. They also extend over all solar latitudes. They were used as tracers of solar rotation since the beginning of the space age (Dupree & Henze 1972). In recent years there are numerous studies investigating solar differential rotation by using CBPs as tracers. Kariyappa (2008); Hara (2009) used Yohkoh/SXT data while Brajša et al. (2001, 2002b, 2004); Vršnak et al. (2003); Wöhl et al. (2010) used SOHO-EIT observations. Kariyappa (2008) also used Hinode/XRT full-disk images to determine the solar rotation profile.

Other tracers are used as well: magnetic fields (Wilcox & Howard 1970; Snodgrass 1983; Komm et al. 1993) and Hα filaments (Brajša et al. 1991). Apart from tracers, Doppler measurements can also be used (Howard & Harvey 1970; Ulrich et al. 1988; Snodgrass & Ulrich 1990).

Helioseismic measurements also show differential rotation below the photosphere all the way down to the bottom of the convective zone (Kosovichev et al. 1997; Schou et al. 1998). Further below, the rotation profile becomes uniform for all latitudes (cf. eg. Howe 2009).

For further details about solar rotation, its importance for solar dynamo models, comparison between different sources see the reviews by Schröter (1985); Howard (1984); Beck (2000); Ossendrijver (2003); Rüdiger & Hollerbach (2004); Stix (2004); Howe (2009); Rozelot & Neiner (2009).

In this work we will use CBP data obtained by SDO/AIA in only two days to assess the quality of the data, identify sources of errors and calculate solar differential rotation profile. We will also investigate the possibility to use CBP data from SDO/AIA for further studies of other related phenomena (meridional flow, rotation velocity residuals and Reynolds stress).

CBP data from SDO/AIA were also used in other works. Lorenc et al. (2012) discussed rotation of the solar corona based on 69 structures from 674 images detected in 9.4 nm channel using an interactive method of detection. Dorotovič et al. (2014) presented a hybrid algorithm for detection and tracking of CBPs. McIntosh et al. (2014b) used detection algorithm presented in their previous paper (McIntosh & Gurman 2005) to identify CBPs in SDO/AIA 19.4 nm channel and correlate their proper-

Send offprint requests to: D. Sudar, e-mail: : davor.sudar@gmail.com

ties with those of giant convective cells. Using more SDO/AIA data and extending analysis back to SOHO era, McIntosh et al. (2014a) concluded that CBPs almost exclusively form around the vertices of giant convective cells.

2. Data and reduction methods

We have used preliminary data from Atmospheric Imaging Assembly (AIA) instrument on board Solar Dynamics Observatory (SDO) satellite (Lemen et al. 2012). The spatial resolution of the instrument is ≈0.6”/pixel. For comparison, SOHO/EIT resolution is 2.629”/pixel while Hinode/XRT has a resolution of 1.032”/pixel.

To obtain positional information of coronal bright points (CBPs) we used the segmentation algorithm which uses the 19.3 nm AIA channel to search for localized, small intensity enhancements in the EUV part of the spectrum compared to the smoothed background intensity. More details about the detection algorithm can be found in Martens et al. (2012) which is based on the algorithm by McIntosh & Gurman (2005).

This resulted in measurements of 66842 positions of 13646 individual CBPs covering two days (1st and 2nd of January 2011). Time interval between two successive images was 10 minutes. In top panel of Fig. 1 we show the distribution of detected CBPs and compare it to the full disk image of the Sun in the 19.3 nm channel obtained on 1st of January 2011 (bottom panel of the same Figure). In the bottom panel white circles show CBPs that were detected on one image by the segmentation algorithm. We can see that CBPs are scarce in active regions, partly because of difficulties in detecting them above such bright areas.

The segmentation algorithm provides coordinates in pixels (centroids of CBPs on the image) and we converted them to heliographic coordinates taking into account current distance of the Sun given in FITS files (Roša et al. 1995, 1998). Positions of objects on the limb of the Sun are fairly inaccurate. Limiting the data to ±58°from the centre of the Sun or ≈0.85$R_\odot$ of the projected solar disk removes this problem (cf. Balthasar et al. 1986).

As can be seen from Fig. 2, calculated velocities show some scatter because the shifts are fairly small in a very short time (10 min). Significant variations in brightness and structure of CBPs also influence calculation of the centroid points. However, trends are visible, especially in azimuthal motion which is known to be a significantly larger effect. That is why we have chosen to approximate the motion with a linear fit to calculate the velocities:

$$\omega_{syn} = \frac{N\sum_{i=1}^{N} l_i t_i - \sum_{i=1}^{N} l_i \sum_{i=1}^{N} t_i}{N\sum_{i=1}^{N} t_i^2 - \left(\sum_{i=1}^{N} t_i\right)^2}, \quad (1)$$

$$\omega_{mer} = \frac{N\sum_{i=1}^{N} b_i t_i - \sum_{i=1}^{N} b_i \sum_{i=1}^{N} t_i}{N\sum_{i=1}^{N} t_i^2 - \left(\sum_{i=1}^{N} t_i\right)^2}, \quad (2)$$

where ω_{syn} is a synodic rotational velocity, ω_{mer} is a meridional angular velocity, l_i is central meridian distance (CMD) and b_i is latitude of each measurement for a single CBP. We have also removed all CBPs which had less than 10 measurements of position in order for linear fits to be more robust. This is equivalent to 100 minutes or about 1°at the equator.

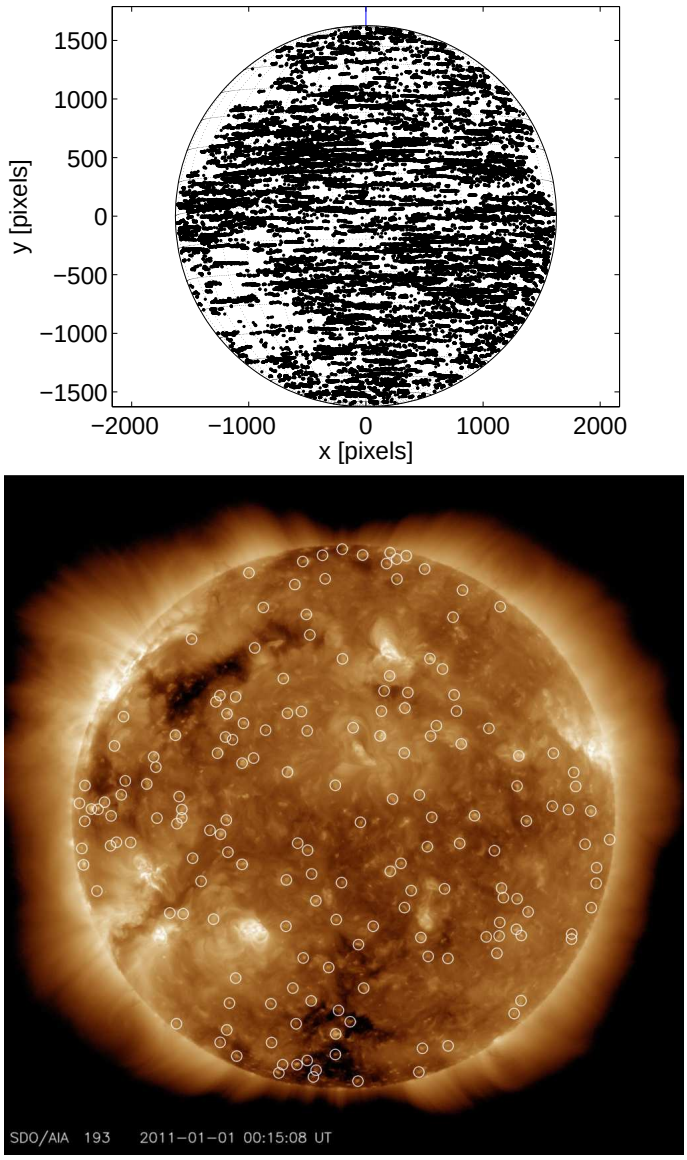

Fig. 1. Distribution of CBPs detected by the segmentation algorithm (top panel) and image of the Sun in the 19.3 nm channel obtained by SDO/AIA on 1st of January 2011. White circles show detected CBPs on this image (bottom panel).

To obtain a true rotation of CBPs on the Sun we need to convert synodic velocities to sidereal. For the transformation we have used Eq. 7 from Skokić et al. (2014).

Trying to identify the same object on subsequent images with an automatic method is bound to result in some misidentification. Resulting velocities are usually very large and can easily be removed by applying a simple filter for velocities Even the human factor can introduce such errors. For example, Sudar et al. (2014) analysed solar rotation residuals and meridional motions of sunspot groups from the Greenwich Photoheliographic Results and found that they have to use a filter $8< \omega_{rot} <19°\text{day}^{-1}$ for rotational velocity in order to eliminate these erroneous measurements. The Greenwich Photoheliographic Results catalogue is being investigated and revised partly in order to remove such problems (Willis et al. 2013a,b; Erwin et al. 2013). In this work we have also used a $8< \omega_{rot} <19°\text{day}^{-1}$ filter for rotational velocities to remove such

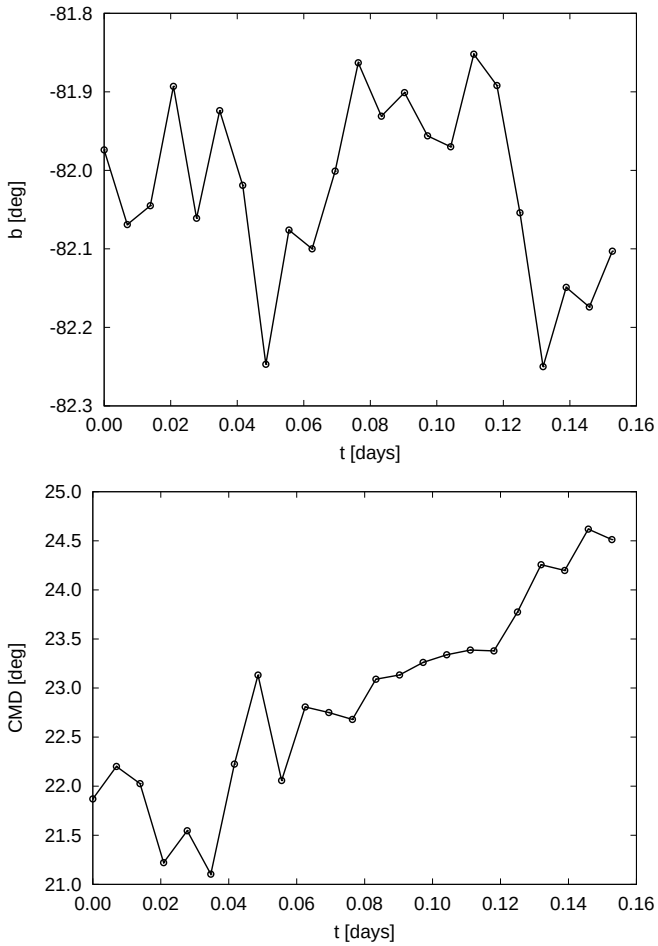

Fig. 2. Motion of a single CBP. Top panel: latitude, b, over time, t; bottom panel: central meridional distance, CMD over time, t.

outliers. In addition we applied a filter -4< ω_{mer} <4°day^{-1} for meridional velocities because it also helps in removing the outliers. Finally, we discarded all the CBPs with less than 10 measurements of position.

After completing all the procedures described above, we had 906 measurements of velocities obtained by tracing CBPs in just two days. Olemskoy & Kitchatinov (2005) pointed out that nonuniform distribution of tracers can result in false flows. This effect is most notable for meridional motion and rotation velocity residuals, but can easily be removed by assigning the calculated velocity to the latitude of the first measurement of position (Olemskoy & Kitchatinov 2005; Sudar et al. 2014). Although the effect is negligible for solar rotation, we want to point out that we applied this correction even for rotation velocity profiles in this work.

Even when the tracers are uniformly distributed over the solar surface, the distribution of tracers over latitude would be nonuniform. As we move from equator to the pole, area of each latitude bin becomes gradually smaller, so we would observe progressively less tracers.

3. Results

In this work we present the motion of CBPs obtained by SDO/AIA instrument. For better understanding of the results and potential of future studies, it is very useful to analyse the accuracy and errors of this dataset.

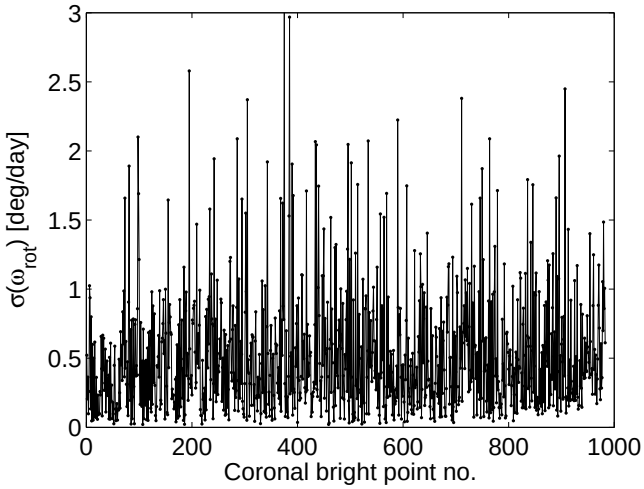

Fig. 3. Errors of rotational velocity, ω_{rot}, for each of the 906 measurements.

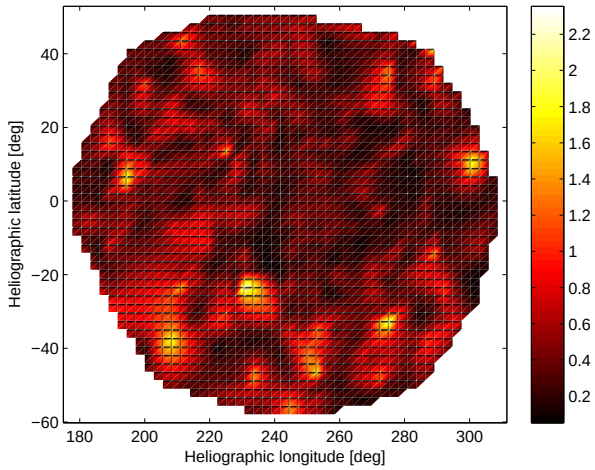

Fig. 4. Distribution of rotation velocity (ω_{rot}) errors in heliographic coordinates. Error scale is in ° day^{-1}.

In Fig. 3 we show errors of the calculated rotational velocities, ω_{rot}, for each CBP obtained with linear fitting of longitude vs time measurements. Although the errors can go up to 3°day^{-1}, the majority is below 1°day^{-1}. In Fig. 4 we show these errors in heliographic coordinates to check their spatial distribution on the solar surface. Larger errors are shown with brighter shades and we can see that larger errors roughly correspond to active regions shown in the bottom panel of Fig. 1. This correlation with active region is probably a consequence of detection algorithm design and difficulties involving detection of CBPs over bright background.

In Fig. 5 we show the distribution of CBPs in heliographic coordinates with arrows showing the velocity vector. As expected, the dominant direction is that of solar rotation.

Latitudinal dependence of rotational velocity is usually expressed as (Howard & Harvey 1970; Schröter 1985):

$$\omega_{rot}(b) = A + B\sin^2 b + C\sin^4 b, \quad (3)$$

where b is the latitude. Parameter A represents equatorial velocity, while B and C depict the deviation from rigid body rotation. The problem with Eq. 3 is that functions in this expression

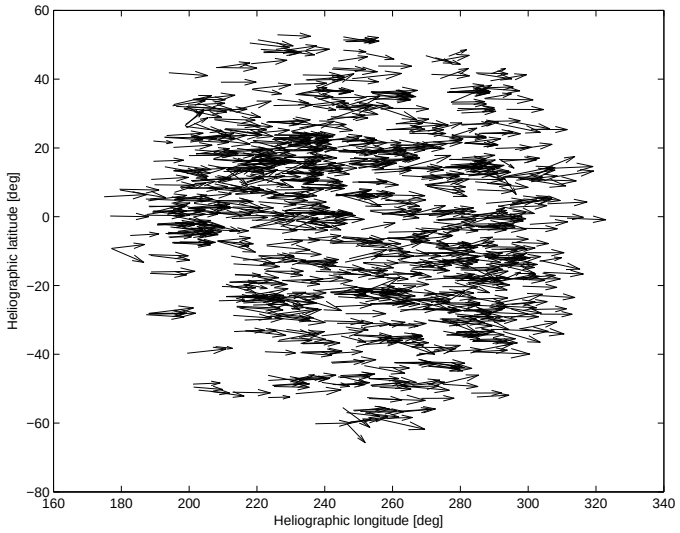

Fig. 5. Distribution of CBPs in heliographic coordinates with arrows showing the direction and strength of the velocity vector.

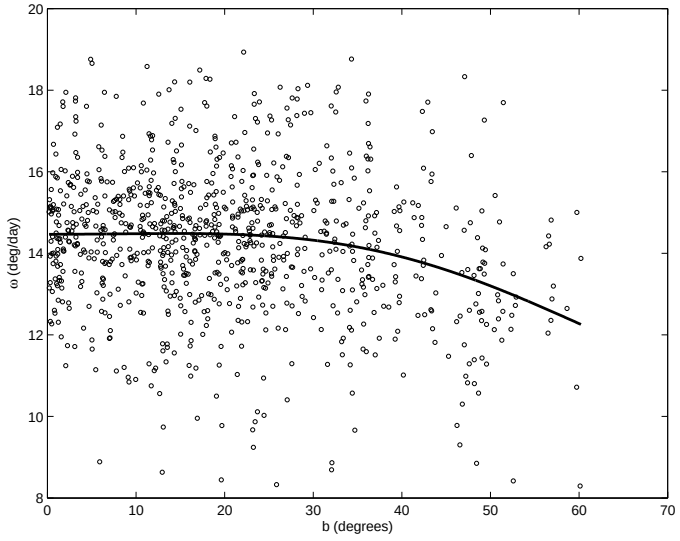

Fig. 6. Solar differential rotation profile obtained with data from SDO/AIA. Open circles are individual measurements, while the solid line is the best fit defined by Eq. 3 for the $A \neq B \neq C$ case.

are not orthogonal so parameters are not independent of each other (Duvall & Svalgaard 1978; Snodgrass 1984; Snodgrass & Howard 1985; Snodgrass & Ulrich 1990). This crosstalk among the coefficients is particularity bad for B and C. The effect of crosstalk does not affect the actual shape of the fit ($\omega_{rot}(b)$), but it creates confusion when directly comparing coefficients from different authors or obtained by different indicators.

To alleviate this problem, frequently the parameter C is set to zero since its effect is noticeable only on higher latitudes. This is almost a standard practise when observing rotation by tracing sunspots or sunspot groups because their positions do not extend to high latitudes (Howard et al. 1984; Balthasar et al. 1986; Pulkkinen & Tuominen 1998; Brajša et al. 2002a; Sudar et al. 2014).

Another method to reduce the crosstalk problem is to set C/B ratio to some fixed value. Scherrer et al. (1980) set the ratio $C/B = 1$ while Ulrich et al. (1988), after measuring the covariance of B and C, set the ratio to $C/B = 1.0216295$.

Table 1. Coefficients of solar rotation profile.

Type	A [°day^{-1}]	B [°day^{-1}]	C [°day^{-1}]	n
A, B, C	14.47±0.10	+0.6±1.0	-4.7±1.7	906
$A, B = C$	14.59±0.07	-1.35±0.21	-1.35±0.21	906
$A, B, C = 0$	14.62±0.08	-2.02±0.33	0	906
Northern hemisphere				
A, B, C	14.43±0.13	+0.8±1.5	-5.6±3.0	461
$A, B = C$	14.55±0.10	-1.35±0.35	-1.35±0.35	461
$A, B, C = 0$	14.57±0.10	-1.92±0.52	0	461
Southern hemisphere				
A, B, C	14.50±0.15	+0.7±1.4	-4.8±2.3	445
$A, B = C$	14.65±0.11	-1.39±0.28	-1.39±0.28	445
$A, B, C = 0$	14.69±0.12	-2.14±0.45	0	445

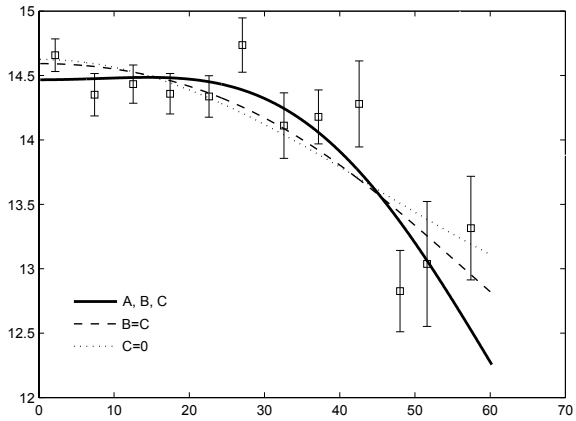

Fig. 7. Comparison of three different fitting procedures for the solar differential rotation profile. Average values of ω_{rot} in 5° bins in latitude, b, are also shown with their respective errors.

In Fig. 6 we show individual measurements of rotational velocities, ω_{rot}, with respect to latitude, b, as open circles. With a solid line we show the result of the best fit to the data of a functional form given in Eq. 3. Coefficients of the fit are given in Table 1. We also fitted the rotation profile for Northern and Southern solar hemisphere separately because of possible asymmetry (cf.eg. Wöhl et al. 2010) and shown the results in the same table. Coefficient A shows a larger value for the Southern hemisphere for all 3 fit functions. Jurdana-Šepić et al. (2011) reported that coefficient A is larger when solar activity is smaller. According to the SIDC data (SILSO World Data Center 2011) we can see that Northern hemisphere is more active both when looking at the monthly smoothed means and daily sunspot data. This fits the findings by Jurdana-Šepić et al. (2011). However, judging by the errors of the coefficients, this difference between South and North is statistically low and the hypothesis that this is a result of asymmetric solar activity needs to be verified with a larger data sample.

In Fig. 7 we show a comparison between different fitting techniques: $A \neq B \neq C$ (solid line), $A \neq B = C$ (dashed line) and $A \neq B, C = 0$ (dotted line). In the same figure we also show average values of ω_{rot} in bins 5° wide in latitude, b, with their respective errors.

4. Discussion

In Table 2 we show a comparison for solar differential profile (Eq. 3) from a number of different sources including the results

Table 2. Comparison with some other results.

Method/object	time period	A [°day^{-1}]	B [°day^{-1}]	C [°day^{-1}]	A_G [°day^{-1}]	B_G [°day^{-1}]	C_G [°day^{-1}]	Ref
CBPs	1967	14.65±0.2			14.65			(1)
CBPs	1994-1997	14.39±0.01	-1.91±0.10	-2.45±0.17	13.80	-0.709	-0.117	(2)
CBPs	1998-1999	14.454±0.027	-2.22±0.07	-2.22±0.07	13.82	-0.740	-0.106	(3)
CBPs	1998-2006	14.499±0.006	-2.54±0.06	-0.77±0.09	13.93	-0.611	-0.037	(4)
CBPs	1-2 Jan 2011	14.47±0.10	+0.6±1.0	-4.7±1.7	14.19	-0.507	-0.224	(5)
CBPs	1-2 Jan 2011	14.59±0.07	-1.35±0.21	-1.35±0.21	14.20	-0.450	-0.064	(5)
CBPs	1-2 Jan 2011	14.62±0.08	-2.02±0.33		14.22	-0.404		(5)
sunspots	1853-1996	14.531±0.003	-2.75±0.05		13.98	-0.550		(6)
sunspots	1874-1976	14.551±0.006	-2.87±0.06		13.98	-0.574		(7)
sunspot groups	1878-2011	14.499±0.005	-2.64±0.05		13.97	-0.528		(8)
sunspot groups	1880-1976	14.37±0.01	-2.59±0.16		13.85	-0.518		(9)
sunspots	1921-1982	14.522±0.004	-2.84±0.04		13.95	-0.568		(10)
sunspot groups	1921-1982	14.393±0.010	-2.95±0.09		13.80	-0.590		(10)
Hα filaments	1972-1987	14.45±0.15	-0.11±0.90	-3.69±0.90	14.11	-0.514	-0.176	(11)
magnetic features	1967-1980	14.307±0.005	-1.98±0.06	-2.15±0.11	13.73	-0.683	-0.102	(12)
magnetic features	1975-1991	14.42±0.02	-2.00±0.13	-2.09±0.15	13.84	-0.679	-0.100	(13)
Doppler	1966-1968	13.76	-1.74	-2.19	13.22	-0.640	-0.104	(14)
Doppler	1967-1984	14.05	-1.49	-2.61	13.53	-0.646	-0.124	(15)

References. (1) Dupree & Henze (1972); (2) Hara (2009); (3) Brajša et al. (2004); (4) Wöhl et al. (2010); (5) this paper; (6) Pulkkinen & Tuominen (1998); (7) Balthasar et al. (1986); (8) Sudar et al. (2014); (9) Brajša et al. (2002a); (10) Howard et al. (1984) (11) Brajša et al. (1991); (12) Snodgrass (1983); (13) Komm et al. (1993); (14) Howard & Harvey (1970); (15) Snodgrass (1984);

from this paper (Table 1). Since we found no statistically significant difference between Northern and Southern hemisphere we only include the results for both hemispheres combined. Results in Table 2 come from a wide variety of different techniques, tracers and instruments.

Snodgrass (1984) suggested that the rotation profile should be expressed in terms of Gegenbauer polynomials since they are orthogonal on the disk. This eliminates the cross-talk problem between coefficients in Eq. 3. Using the expansion in terms of Gegenbauer polynomials solar rotation profile becomes:

$$\omega_{rot}(b) = A_G T_0^1(\sin b) + B_G T_2^1(\sin b) + C_G T_4^1(\sin b), \quad (4)$$

where A_G, B_G and C_G are coefficients of expansion and $T_0^1(\sin b)$, $T_2^1(\sin b)$ and $T_4^1(\sin b)$ are Gegenbauer polynomials as defined by Snodgrass & Howard (1985) in their equation (2).

As Snodgrass & Howard (1985); Snodgrass & Ulrich (1990) pointed out, the relationship between coefficients A, B and C from standard rotation profile (Eq. 3) and coefficients A_G, B_G and C_G from Eq. 4 is linear. Therefore, it is not necessary to recalculate the fits with expansion to Gegenbauer polynomials, we can just calculate A_G, B_G and C_G from A, B and C. We used the relationship given in Snodgrass & Howard (1985) (their equation (4)) since there seems to be a typo for a similar relationship for coefficients C and C_G in Snodgrass & Ulrich (1990). In Table 2 we also show the values of coefficients A_G, B_G and C_G.

Results in this paper roughly match all other previously published works. The accuracy of coefficients is lower when compared with other results which is a consequence of fairly small number of data points ($n = 906$). For example Wöhl et al. (2010) had more than 50000 data points in the time interval of 8 years. However, we used the data spanning only 2 days. It is conceivable that with AIA/SDO CBP data we could reach 50000 data points in only 4 months and achieve similar accuracy in solar rotation profile coefficients. This means that with AIA/SDO data it is possible to measure rotation profile several times per year and track possible changes in solar surface differential rotation directly with a very simple tracer method. This is also true for meridional motion and Reynolds stress, both of which probably vary within the solar cycle (cf. e.g Sudar et al. 2014).

5. Summary and Conclusion

Using preliminary results from SDO/AIA instrument we identified a large number of CBPs which resulted in 906 rotation velocity measurements. We obtained a fairly good differential solar rotation profile in spite of the fact that we used data from two days only.

CBPs are also very good tracers since they extend to much higher latitudes than sunspots. They are also quite numerous in all phases of the solar cycle while sunspots are often absent in the minimum of the cycle.

We will also investigate the potential of preliminary SDO/AIA CBP data to determine meridional motions, rotation velocity residuals, Reynolds stresses and diffusion in subsequent papers.

It is quite conceivable that errors of the differential rotation profile coefficients would drop significantly when more data is used. From our analysis, we can expect to obtain 400-500 velocity measurements per day. Time interval of 4 months seems adequate to obtain 50000 velocity measurements which should be sufficient to match the most accurate results obtained by tracer methods (for example Wöhl et al. (2010)). Moreover, the spatial resolution of SDO/AIA is better than comparable instruments (SOHO/EIT and Hinode/XRT).

This opens up an intriguing possibility to measure solar rotation profile almost from one month to the next. Such studies could provide new insight into mechanisms responsible for solar rotation. We already know that meridional motion exhibits some changes during the course of the solar cycle and the same is probably true for Reynolds stress. Sudar et al. (2014) found by averaging almost 150 years of sunspot data that meridional motion is slightly changing within the solar cycle and hinted that the Reynolds stresses are probably changing too. We have also found a small asymmetry in rotation profile for two solar hemispheres and suggested that this might be related to different solar activity on the hemispheres. This needs to be verified with a larger dataset because difference in rotation profiles are of low statistical significance. Having more detailed temporal resolu-

tion and direct results (without the need to average many solar cycles) could prove to be very informative.

Planned SDO mission duration of 5–10 years will cover a large portion of the solar cycle which would result in enormous amount of velocity data and help in understanding the nature of solar rotation profile.

Time interval of 10 minutes between successive images also offers a good opportunity to study the evolution of CBPs and possible effect this might have on detected solar surface velocity fields. For example Vršnak et al. (2003) reported that longer lasting CBPs show different results than short-lived CBPs.

Acknowledgements. This work has received funding from the European Commission FP7 project eHEROES (284461, 2012-2015) **and SOLARNET project (312495, 2013-2017) which is an Integrated Infrastructure Initiative (I3) supported by FP7 Capacities Programme. It was also supported by Croatian Science Foundation under the project 6212 Solar and Stellar Variability.** SS was supported by NASA Grant NNX09AB03G to the Smithsonian Astrophysical Observatory and contract SP02H1701R from Lockheed-Martin to SAO. We would like to thank SDO/AIA science teams for providing the observations. We would also like to thank Veronique Delouille and Alexander Engell for valuable help in preparation of this work.

References

Balthasar, H., Vázquez, M., & Wöhl, H. 1986, A&A, 155, 87
Beck, J. G. 2000, Sol. Phys., 191, 47
Brajša, R., Vršnak, B., Ruždjak, V., Schroll, A., & Pohjolainen, S. 1991, Sol. Phys., 133, 195
Brajša, R., Wöhl, H., Vršnak, B., et al. 2002a, Sol. Phys., 206, 229
Brajša, R., Wöhl, H., Vršnak, B., et al. 2001, A&A, 374, 309
Brajša, R., Wöhl, H., Vršnak, B., et al. 2002b, A&A, 392, 329
Brajša, R., Wöhl, H., Vršnak, B., et al. 2004, A&A, 414, 707
Dorotovič, I., Shahamatnia, E., Lorenc, M., et al. 2014, Sun and Geosphere, 9, 81
Dupree, A. K. & Henze, Jr., W. 1972, Sol. Phys., 27, 271
Duvall, Jr., T. L. & Svalgaard, L. 1978, Sol. Phys., 56, 463
Erwin, E. H., Coffey, H. E., Denig, W. F., et al. 2013, Sol. Phys., 288, 157
Hara, H. 2009, ApJ, 697, 980
Howard, R. 1984, ARA&A, 22, 131
Howard, R., Gilman, P. I., & Gilman, P. A. 1984, ApJ, 283, 373
Howard, R. & Harvey, J. 1970, Sol. Phys., 12, 23
Howe, R. 2009, Living Reviews in Solar Physics, 6, 1
Jurdana-Šepić, R., Brajša, R., Wöhl, H., et al. 2011, A&A, 534, A17
Kariyappa, R. 2008, A&A, 488, 297
Komm, R. W., Howard, R. F., & Harvey, J. W. 1993, Sol. Phys., 145, 1
Kosovichev, A. G., Schou, J., Scherrer, P. H., et al. 1997, Sol. Phys., 170, 43
Lemen, J. R., Title, A. M., Akin, D. J., et al. 2012, Sol. Phys., 275, 17
Lorenc, M., Rybanský, M., & Dorotovič, I. 2012, Sol. Phys., 281, 611
Martens, P. C. H., Attrill, G. D. R., Davey, A. R., et al. 2012, Sol. Phys., 275, 79
McIntosh, S. W. & Gurman, J. B. 2005, Sol. Phys., 228, 285
McIntosh, S. W., Wang, X., Leamon, R. J., et al. 2014a, ApJ, 792, 12
McIntosh, S. W., Wang, X., Leamon, R. J., & Scherrer, P. H. 2014b, ApJ, 784, L32
Newton, H. W. & Nunn, M. L. 1951, MNRAS, 111, 413
Olemskoy, S. V. & Kitchatinov, L. L. 2005, Astronomy Letters, 31, 706
Ossendrijver, M. 2003, A&A Rev., 11, 287
Pulkkinen, P. & Tuominen, I. 1998, A&A, 332, 755
Roša, D., Vršnak, B., & Božić, H. 1995, Hvar Observatory Bulletin, 19, 23
Roša, D., Vršnak, B., Božić, H., et al. 1998, Sol. Phys., 179, 237
Rozelot, J.-P. & Neiner, C., eds. 2009, Lecture Notes in Physics, Berlin Springer Verlag, Vol. 765, The Rotation of Sun and Stars
Rüdiger, G. & Hollerbach, R. 2004, The Magnetic Universe, by G. Rüdiger and R. Hollerbach. ISBN 3-527-40409-0. Wiley Interscience, 2004.
Scherrer, P. H., Wilcox, J. M., & Svalgaard, L. 1980, ApJ, 241, 811
Schou, J., Antia, H. M., Basu, S., et al. 1998, ApJ, 505, 390
Schröter, E. H. 1985, Sol. Phys., 100, 141
SILSO World Data Center. 2011, International Sunspot Number Monthly Bulletin and online catalogue
Skokić, I., Brajša, R., Roša, D., Hržina, D., & Wöhl, H. 2014, Sol. Phys., 289, 14711476
Snodgrass, H. B. 1983, ApJ, 270, 288
Snodgrass, H. B. 1984, Sol. Phys., 94, 13
Snodgrass, H. B. & Howard, R. 1985, Sol. Phys., 95, 221
Snodgrass, H. B. & Ulrich, R. K. 1990, ApJ, 351, 309
Stix, M. 2004, The sun : an introduction, 2nd ed., by Michael Stix. Astronomy and astrophysics library, Berlin: Springer, 2004. ISBN: 3540207414
Sudar, D., Skokić, I., Ruždjak, D., Brajša, R., & Wöhl, H. 2014, MNRAS, 439, 2377
Ulrich, R. K., Boyden, J. E., Webster, L., Padilla, S. P., & Snodgrass, H. B. 1988, Sol. Phys., 117, 291
Vršnak, B., Brajša, R., Wöhl, H., et al. 2003, A&A, 404, 1117
Wilcox, J. M. & Howard, R. 1970, Sol. Phys., 13, 251
Willis, D. M., Coffey, H. E., Henwood, R., et al. 2013a, Sol. Phys., 288, 117
Willis, D. M., Henwood, R., Wild, M. N., et al. 2013b, Sol. Phys., 288, 141
Wöhl, H., Brajša, R., Hanslmeier, A., & Gissot, S. F. 2010, A&A, 520, A29